LIGHT-SCATTERING SPECTRUM

DUE TO WIGGLING MOTIONS OF BACTERIA

JEAN PIERRE BOON, RALPH NOSSAL, *and* SOW-HSIN CHEN

From the Department of Nuclear Engineering and Department of Chemistry,
Massachusetts Institute of Technology, Cambridge, Massachusetts 02139, and the
Physical Sciences Laboratory, Division of Computer Research and Technology,
National Institutes of Health, Bethesda, Maryland 20014. Dr. Boon's present address is
Faculté des Sciences, Université Libre de Bruxelles, 1050 Brussels, Belgium.

ABSTRACT   Simple models are used to calculate the inelastic light scattering spectrum of motile bacteria when wiggling motions are included in addition to translational displacement. Computations of spectra lead to the conclusion that nontranslational motions can be neglected when swimming speeds are deduced from light-scattering data for normal vigorously motile strains. On the other hand, for slowly translating bacteria, or for strains exhibiting noticeable wiggling motion when viewed in a microscope, additional spectral components may be significant. Such components are best distinguished when measurements are made at small and intermediate scattering angles; at large angles the spectra have approximately the same scaling properties (functionals of Qt, Q being the Bragg wave vector) as those associated with simple translational motility.

I. INTRODUCTION

Using a unique tracking microscope, Berg and Brown (1, 2) recently investigated details of the trajectories of certain strains of flagellated *E. coli* bacteria. They found that a bacterium typically follows a linear path for a distance approximately 10 times its length, after which it quivers (tumbles or "twiddles") and then changes direction. For wild-type bacteria moving in spatially homogeneous media, the time spent in "twiddling" can be as much as 15% of the total trajectory time. However, considerably less twiddling is observed in the motions of nonchemotactic mutants, suggesting that such movements are related to the detection of chemoattractant gradients. Additional evidence for correlations between chemotactic response and nontranslational motions of bacteria appears in the studies of Macnab and Koshland (3) and Tsang et al. (4), which indicate that tumbling occurs to a greater extent when bacteria move from regions of high to low chemoattractant concentration.

Methods of laser light intensity correlation spectroscopy recently have been used to measure translational velocities of motile bacteria (5-7). Since bacterial dimensions are of the same order as the wavelength of the incident light, spectral components due to wiggling and twisting motions also may be observable. These motions are promi-

nent under certain conditions (e.g., "overgrowth" of the culture, the addition of ~ 10% glycerol, genetically abnormal motility), although in previously reported studies (5, 7), samples were prepared such that bacterial motion visually could be characterized as primarily straight line translation. Our purpose, here, is to investigate the possibility of developing quantitative measures of the wiggling and twisting modes of swimming microorganisms. Additionally, we wish to assure ourselves that errors will not be made if translational velocities are deduced from the spectra when bacteria are moving with a minimum of observable nontranslational components (7).

In previous publications, it was implied that a useful first approximation to the light-scattering spectrum of motile organisms is obtained by considering the particles to be point scatterers moving with constant velocities for times which are long compared with typical spectral decay times. In such case, the correlation function $I(Q, t)$, which is the time Fourier transform of the light scattering spectrum, is given as (5)

$$I(Q, t) = \int_0^\infty \frac{\sin(QVt)}{QVt} P_s(V) dV \qquad (1)$$

when normalized such that $I(Q, 0) = 1$. Here, $P_s(V)$ is the distribution of swimming speeds, t is the time, and Q is the magnitude of the Bragg wave vector ($Q = 4\pi n\lambda^{-1} \sin(\theta/2)$, where θ is the scattering angle, n is the refractive index of the medium through which the bacteria are moving, and λ is the wavelength of the incident light. Note that Eq. 1 predicts that data taken at different scattering angles would all superimpose when plotted as a function of the reduced variable $x = Qt$. Spectral components due to wiggling motions could appear as deviations from this ideal behavior.

Of course, the gross dimensions of most bacteria are comparable to or larger than the wavelength of visible light. Although the expression given by Eq. 1 might be expected to hold for large particles if they are spherically symmetric, there is no a priori reason to assume that it pertains to rod-shaped bacteria such as E. coli. In a companion publication (8) we show that computed correlation functions for non-wiggling motile rods present significant deviations from Eq. 1 when the velocities of the particles are assumed to lie parallel to their long axes.

On the other hand, scaling according to Eq. 1 seems to be observed when care is taken to prepare a sample of bacteria that do not wiggle (5). This paradox can be resolved when it is recognized that bacteria are optically heterogeneous, i.e. that they contain internal structures whose polarizabilities differ from that of the exterior region of the cell. Insofar as light scattering is concerned, the effective size of a bacterium might be much smaller than its geometric size. Concomitant differences in shape also must be considered.

Indeed, phase contrast microscopy of E. coli bacteria oftentimes shows opaque regions ("chromatinic bodies") which occupy only part of the cell volume (9, 10). These structures, which are believed to be analogs of the nuclear regions of eukaryotic cells,

have somewhat irregular shapes and seem to be randomly oriented with respect to the cell axes (10). The net effect is that the chromatinic bodies may be treated as presenting a morphology which is nearly spherical when averaged over the various orientations. The chromatinic bodies also can be visualized by histochemical techniques (11, 12) and electron microscopy (12, 13). Various studies show that the shapes of the nucleoid bodies change according to culture conditions (9, 11). For bacteria in log-phase growth, the chromatin-rich regions usually appear in pairs localized at the opposite ends of a bacterium; however, when growth is inhibited the bacteria appear to contain only one chromatinic body (9, 13). The nucleoid bodies form compact "condensed" masses when culture conditions are maintained properly, such that the bacteria can regulate their internal ionic environments (11, 13).

Inelastic light scattering from internally structured particles has been analyzed in ref. 8, where it has been shown that coherent interference of the scattering from different parts of a complex particle can have important effects on the resulting spectra. Internal structures can scatter light with relatively greater intensity than can the exterior regions of the particles, given that the internal regions have a relatively more isotropic shape and provided that their indices of refraction are sufficiently different from that of the exterior region.

The basic model of ref. 8 is a particle having ellipsoidal Gaussian mass distributions, primary attention being focused there on the consequences of particle anisotropies. In this paper, on the other hand, we principally are concerned with spectral effects due to off-axial wiggling motions; we compute correlation functions for some simpler distributions of scattering mass which, while roughly representing complicated internal structures, yet are amenable to mathematical analysis.

In Sec. II we analyze a dumbbell-like model represented by two separated point scatterers which move coherently. When nontranslational movements are absent the spectra derived from this model are equivalent to those from a rigid bacterium containing two identical, spherically symmetric, scattering regions (8). This model can be solved in closed form, and the methodology developed for this purpose then forms the basis of subsequent investigation of spectral components arising from twisting motions. In Sec. III we further analyze the dumbbell model to obtain expressions for spectral modulation arising from off-axial movements.

We present these dumbbell calculations first because, once the mathematics for the more complicated problem has been set forth, analogous results for a single, medially located, wiggling point scatterer may be obtained as a special case. The latter model pertains to a uninucleate cell containing a spherically symmetric nucleoid. Results are given in Sec. IV, along with some for a wiggling line of scattering centers. Such a distributed source might represent a cell whose single chromatinic body is elongated and not spherical. In Sec. V we discuss the results and present some confirming data. Throughout the paper we implicitly assume that the bacteria are in such dilute suspension that they move independently of each other, and that multiple scattering of photons can be neglected.

II. LIGHT SCATTERING SPECTRUM DUE TO A MOTILE TWO-POINT DUMBBELL

To calculate the spectrum we first consider a bacterium to be divided into N linearly distributed segments, and designate $\mathbf{R}(t)$ to be the position of the center of mass of the bacterium and σ_j to be the distance from the center of mass to the center of the jth segment. Since bacteria move without interruption for times which are, on the average, long compared with a typical spectral decay time (5), we may express $\mathbf{R}(t)$ approximately as $\mathbf{R}(t) = \mathbf{R}(0) + V\hat{\mathbf{v}}t$, where $\mathbf{R}(0)$ is the position of the center of mass at $t = 0$ (chosen arbitrarily) and V and $\hat{\mathbf{v}}$ are, respectively, the speed and a unit vector signifying the direction of bacterial translation. Assuming, first, that the bacterium moves with its axis always parallel to $\hat{\mathbf{v}}$, the position of the jth segment may be expressed as $\mathbf{r}_j = \mathbf{R} + \sigma_j \hat{\mathbf{v}}$. Thus, the scattering spectrum may be expressed (14) in terms of the correlation function

$$C(Q, t) = \frac{1}{N^2} \left\langle \left[\sum_{l=1}^{N} a_l \exp[i\mathbf{Q} \cdot \mathbf{r}_l(t)] \right] \left[\sum_{m=1}^{N} a_m \exp[-i\mathbf{Q} \cdot \mathbf{r}_m(0)] \right] \right\rangle$$

$$= \frac{1}{N^2} \left\langle \sum_{l=1}^{N} \sum_{m=1}^{N} a_l a_m \exp[i(\sigma_l - \sigma_m + Vt)\mathbf{Q} \cdot \hat{\mathbf{v}}] \right\rangle, \quad (2)$$

where a_j is the scattering power (the "excess" polarizability) of the jth segment. The brackets $\langle \ldots \rangle$ signify averaging over the velocity distribution of the bacteria. $\mathbf{Q}$ is the Bragg scattering vector (see Eq. 1 ff). To obtain Eq. 2 we have implicitly assumed that Rayleigh-Debye scattering theory is applicable; recent measurements of the total intensity of light scattered by E. coli bacteria are in substantial agreement with this assumption (15).

If all segments were alike ($a_j = a$ for all j), Eq. 2 would pertain to an infinitely thin, optically uniform rod. On the other hand, in accord with the remarks made above in Sec. I, we here consider the scattering mass to be localized at only two points. If the separation between the points is designated as d, Eq. 2 becomes (cf. Eq. 16, below)

$$C(Q, t) = \frac{a^2}{2} \left\langle e^{i\mathbf{Q} \cdot \hat{\mathbf{v}} Vt} [1 + \cos([\mathbf{Q} \cdot \hat{\mathbf{v}}]d)] \right\rangle \quad (3)$$

$$= \frac{a^2}{2} \left\{ 2\pi \int_0^\infty V^2 P(V) dV \int_{-1}^1 d\chi \cos(QVt\chi)[1 + \cos(Q\chi d)] \right\}. \quad (4)$$

In Eq. 4, integration over χ (which represents the cosine of the angle between $\mathbf{Q}$ and $\hat{\mathbf{v}}$) is easily performed. When the resulting correlation function is normalized to unity at $t = 0$, we thus find

$$I_{db}(Q, t) \equiv C(Q, t)/C(Q, 0)$$

$$= [1 + j_0(Qd)]^{-1} \{ \langle j_0(QVt) \rangle + \frac{1}{2} [\langle j_0(Q[Vt + d]) \rangle + \langle j_0(Q[Vt - d]) \rangle] \}, \quad (5)$$
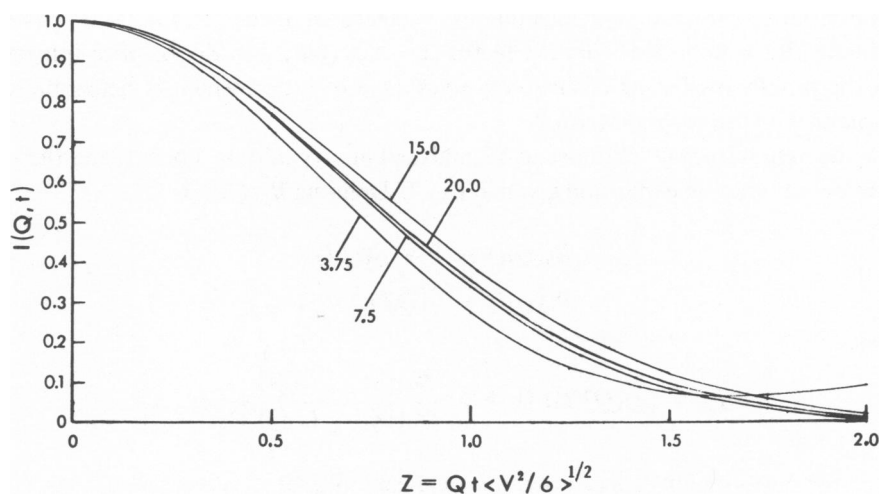
FIGURE 1 Calculated normalized intensity correlation functions $I(Q,t)$ for a translating two-point dumbbell, calculated according to Eqs. 5 and 6. Curves have been computed for different values of the parameter $\varphi = Qd/2$, where Q is the magnitude of the Bragg scattering vector, and d is the distance between the centers of the dumbbells ($\varphi = 3.75, 7.5, 15.0, 20.0$).

where $j_\mu(z)$ is a spherical Bessel function of order μ. Here, $Q = |\mathbf{Q}|$ symbolizes the magnitude of the Bragg vector, and the brackets $\langle...\rangle$ now imply averaging with respect to the bacterial speed distribution, i.e.,

$$\langle j_k(QVt)\rangle = \int_0^\infty j_k(QVt)P_s(V)dV, \tag{6}$$

where $P_s(V) = 4\pi V^2 P(V)$ is the "swimming speed distribution" (5).

An alternate expression for $I_{db}(Q,t)$ is obtained by employing the expansion (16) $j_0(\lambda + \zeta) = \sum_{n=0}^\infty (2n + 1)j_n(\lambda)j_n(\zeta)$, from which one obtains

$$I_{db}(Q,t) = \langle j_0(QVt)\rangle + [1 + j_0(Qd)]^{-1} \sum_{n=1}^\infty (4n + 1)j_{2n}(Qd)\langle j_{2n}(QVt)\rangle. \tag{7}$$

(The odd terms drop out of the series since $j_k(z) = -j_k(-z)$, $k = 1, 3, 5, ...$)

In Fig. 1 we show $I_{db}(Q, t)$ as calculated from Eq. 5. We took the swimming speed distribution $P_s(V)$ to have a Gaussian form, viz.,

$$P_s(V) = (2\alpha/\sqrt{\pi})(\alpha V/2)^2 \exp\{-(\alpha V/2)^2\}, \tag{8}$$

where α is defined as $\alpha = (6/\langle V^2\rangle)^{1/2}$, with $\langle V^2\rangle^{1/2}$ being the root mean square (rms) speed of the bacteria. The curves have been computed for different values of $\varphi = Qd/2$; for reference, we note that, if a He-Ne laser is used, when d is taken as 1.5 μm the parameter value $\varphi \approx 7.5$ implies a scattering angle of approximately 45°. Particu-

larly for large values of Qd, scaling of $I_{db}(Q, t)$ as given in Eq. 1 is observed. (Actually, this is apparent from the factor $[1 + \cos(Qd\chi)]$ in Eq. 4, since integration over the rapidly oscillating cosine term gives a contribution which is negligible when compared with the constant term.)

The deviation from Qt scaling can be analyzed analytically by considering the terms of the Bessel function expansion given in Eq. 7. Defining $B_k(Qd)$ as

$$B_0(Qd) = 1 + j_0(Qd)$$
$$B_k(Qd) = j_k(Qd), \quad k \neq 0,$$

(9)

we have

$$I_{db} = \langle j_0(QVt) \rangle \left\{ 1 + 5 \cdot \frac{B_2(Qd)}{B_0(Qd)} \cdot \frac{I_2(QVt)}{I_0(QVt)} + \ldots \right\},$$

(10)

where, for the swimming speed distribution given in Eq. 8,

$$I_0 \equiv \langle j_0(QVt) \rangle = \exp\{-(Qt/\alpha)^2\},$$

(11)

and

$$I_2 \equiv \langle j_2(QVt) \rangle = \frac{3\sqrt{\pi}}{4} \left(\frac{\alpha}{Qt}\right)^3 \mathrm{erf}\left(\frac{Qt}{\alpha}\right) - \left[1 + \frac{3}{2}\left(\frac{\alpha}{Qt}\right)^2\right] \exp\left\{-\left(\frac{Qt}{\alpha}\right)^2\right\}.$$

(12)

Here, $\mathrm{erf}(\ldots)$ is the error function, viz., $\mathrm{erf}(x) = 2\pi^{-1/2} \int_0^x \exp(-y^2)dy$.
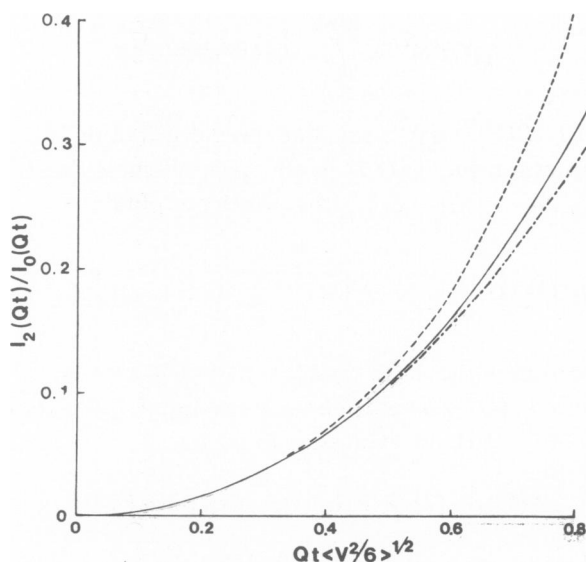

FIGURE 2 The ratio $I_2(Qt)/I_0(Qt)$, evaluated for different swimming speed distributions $P_s(V)$ (see Eqs. 11 and 12). Key: ————— Gaussian distribution; — — — — uniform distribution; ----------- δ-function distribution.

The ratio I_2/I_0, calculated with the distribution given in Eq. 8, is presented in Fig. 2. For comparison, we also show results which are obtained when $P_s(V)$ is uniformly distributed up to a value V_m. (In this case we find $I_0 \equiv \langle j_0(QVt) \rangle = \mathrm{Si}(QV_mt)/QV_mt$, and $I_2 \equiv \langle j_2(QVt) \rangle = [\mathrm{Si}(QV_mt) - 3j_1(QV_mt)]/2QV_mt$; V_m is chosen to be $3^{1/2}$ times the value of the corresponding rms speed. Si (...) is the sine integral [16].) Similarly, we show I_2/I_0 when $P_s(V)$ is δ-function distributed. We observe that, for values of QVt such that $I(Q, t) \gtrsim 0.5$, the ratio I_2/I_0 seems not to depend too strongly upon the specific form of $P_s(V)$.

The other factor in Eq. 10, namely, the ratio $B_2(Qd)/B_0(Qd)$, is less than $(2Qd)^{-1}$ when Qd is large. Taking as an example $\varphi = 7.5$, we find that the first order correction term is negligible, being $5 \cdot (B_2/B_0) \cdot (I_2/I_0) = (5) \cdot (1/30) \cdot (0.3) \simeq 0.05$ at the half-decay point of $I_{db}(Q, t)$. (The value $I_2/I_0 = 0.3$ is taken from Fig. 2, and corresponds to $Qt\langle V^2 \rangle^{1/2} = 2$.) The higher order terms in Eq. 10 are yet smaller, and the series converges rapidly.

III. SPECTRA DUE TO WIGGLING MOTIONS

To assess the spectral perturbations due to wiggling, we again evaluate Eq. 2 for a two-point mass distribution. However, instead of assuming that a bacterium always moves with its axis parallel to its translational velocity, we now also allow for changes in the inclination of the bacterium in relation to the translational direction. To account for this in a simple way, we consider wiggling motion to occur in a plane, with the bacterium moving as if hinged at its head (see Fig. 3). We expect that results are not significantly different in the corresponding three-dimensional case (i.e. we pre-
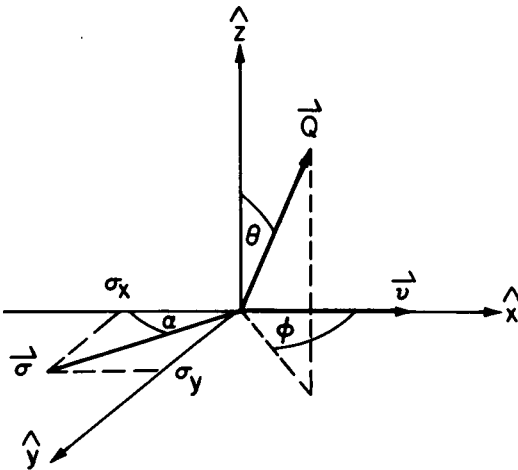

FIGURE 3 Coordinate system used for evaluating Eq. 2 when nontranslational movements are considered. The direction of motion of the bacterium is taken as $\hat{x}$, and the plane of wiggling motion is defined by the coordinates $\{\hat{x}, \hat{y}\}$. The angle of inclination of the bacterium is $\alpha(t)$.

sume that sinusoidal and helical motions give rise to qualitatively equivalent spectral features).

We find it convenient to fix the $\hat{x}$ axis to be in the translational direction of motion of the bacterium and average over the possible orientations of $\mathbf{Q}$ relative to this axis. Let $\alpha(t)$ be the angle between $\hat{\sigma}(t)$ and the direction of motion. In this coordinate system the components of $\hat{\sigma}$ and $\mathbf{Q}$ are then given as (see Fig. 3)

$$\hat{\sigma}(t) = \{-\cos\alpha(t); \sin\alpha(t); 0\}, \tag{13}$$

and

$$\mathbf{Q} = \{Q\sin\theta\cos\varphi; Q\sin\theta\sin\varphi; Q\cos\theta\}. \tag{14}$$

It follows that $C(Q, t)$ may be expressed as

$$C(Q, t) = \frac{1}{4\pi}\left\langle \int_0^\pi d\theta\sin\theta \int_0^{2\pi} d\varphi e^{iQVt\sin\theta\cos\varphi} B_t(Qd \mid \varphi; \theta)\right\rangle, \tag{15}$$

where the brackets $\langle\ldots\rangle$ now signify averaging with respect to the distribution of $\alpha(t)$ and $\alpha(0)$ as well as $P_s(V)$. In Eq. 15, $B_t(Qd \mid \varphi; \theta)$ is defined as

$$B_t(Qd \mid \varphi; \theta) = \frac{1}{4}\{1 + \exp[idQ\sin\theta\cos(\varphi + \alpha(0))]$$

$$+ \exp[-idQ\sin\theta\cos(\varphi + \alpha(t))]$$

$$+ \exp(2idQ\sin[\frac{1}{2}(\alpha(t) - \alpha(0))]$$

$$\cdot\sin\theta\sin[\varphi + \frac{1}{2}(\alpha(t) + \alpha(0))])\} \tag{16}$$

To derive Eq. 16 we have used various trigonometric identities; for example, the fourth term follows from Eqs. 2, 13, and 14 by $[\sin\varphi\cdot(\sin\alpha(t) - \sin\alpha(0)) - \cos\varphi\cdot(\cos\alpha(t) - \cos\alpha(0))] = 2\sin\frac{1}{2}(\alpha(t) - \alpha(0)\cdot\sin(\varphi + \frac{1}{2}(\alpha(t) + \alpha(0))$.

The φ, θ integrals in Eq. 15 can be performed by noting that (16)

$$\int_0^{2\pi} \exp\{iZ\sin\theta\sin(\varphi + \varphi')\}d\varphi = 2\pi J_0(Z\sin\theta) \tag{17}$$

and

$$2\pi \int_0^\pi \sin\theta J_0(Z\sin\theta)d\theta = 4\pi j_0(Z). \tag{18}$$

Thus, Eqs. 15 and 16 may be expressed as (see Appendix A)

$$C(Q, t) = \frac{1}{4}\Big\{\langle j_0(QVt)\rangle + \langle j_0(Q[d^2 + 2Vtd\cos\alpha(0) + (Vt)^2]^{1/2})\rangle$$

$$+ \langle j_0(Q[d^2 - 2Vtd\cos\alpha(t) + (Vt)^2]^{1/2})\rangle \tag{19}$$

$$+ \langle j_0(Q[\beta_t^2 d^2 + 2Vt\beta_t d\sin\frac{1}{2}(\alpha_t + \alpha_0) + (Vt)^2]^{1/2})\rangle\Big\},$$

where β_t represents

$$\beta_t \equiv 2\sin[\tfrac{1}{2}(\alpha(t) - \alpha(0))].\tag{20}$$

Note that, $\lim_{d\to 0} C(Q, t) = \langle j_0(QVt)\rangle$, i.e., when a particle is small compared with the wavelength of the incident light, wiggle motions will not be discernible. Similarly, if the wiggle amplitude is small (i.e. $\alpha(t) \approx 0$), the expression given in Eq. 19 tends to that given in Eq. 5.

Eq. 19 could be used for computations. However, our current purposes are better served by first employing an addition theorem for the Bessel functions, similar to that which we used to derive Eqs. 7 and 10. We have (16)

$$j_0([\rho^2 + r^2 - 2\rho r\cos\theta]^{1/2}) = \sum_{n=0}^{\infty} (2n + 1)j_n(\rho)j_n(r)P_n(\cos\theta),\tag{21}$$

where the $P_n(\cdot\cdot\cdot)$ are Legendre polynomials. Thus, Eq. 19 becomes

$$C(Q,t) = \frac{1}{4}\langle 1 + 2j_0(Qd) + j_0(Q\beta_t d)\rangle\langle j_0(QVt)\rangle$$

$$- \frac{3}{4}\langle\sin\tfrac{1}{2}[\alpha(t) + \alpha(0)]\{j_1(Qd\beta_t) + \beta_t j_1(Qd)\}\rangle\langle j_1(QVt)\rangle$$

$$+ \cdot\cdot\cdot\cdot\tag{22}$$

When the first order correction term is examined, we note that if $\alpha(t)$ is small, the term $B_1(t) \equiv [j_1(Qd\beta_t) + \beta_t j_1(Qd)]\sin([\alpha(t) + \alpha(0)]/2)$ is of order $\mathcal{O}(\alpha^2)$. Also, if Qd is large but $\alpha(t)$ not small, then $B_1(t) \sim \mathcal{O}(0.5/Qd)$. Consequently, as an extension of the arguments used to show that Eq. 10 approximates Eq. 7, we keep only the first term in Eq. 22 and now write

$$I_{db}^w(Q,t) \simeq f_{db}^w(Q,t)\langle j_0(QVt)\rangle,\tag{23}$$

where the normalized function

$$f_{db}^w(Q,t) = \{1 + 2j_0(Qd) + \langle j_0(Q\beta_t d)\rangle\}/[2 + 2j_0(Qd)]\tag{24}$$

pertains to the spectral modulation due to the nontranslational wiggling and wobbling of the dumbbell model.

In Eq. 24, the expectation $\langle\ldots\rangle$ refers to averaging with respect to the stochastic variable $\alpha(t)$. To our knowledge, wiggling motions have not yet been studied systematically, and we thus choose the simple functional form
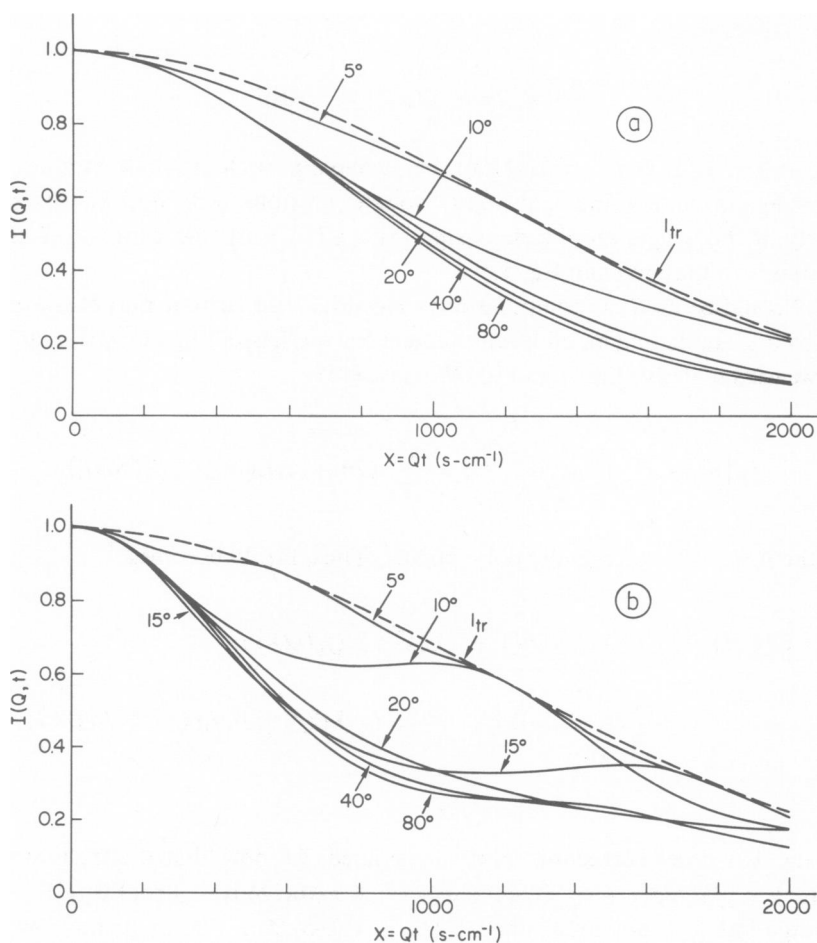
$$\alpha(t) = A\sin w_0 t\tag{25}$$

FIGURE 4   Normalized intensity correlation functions $I_{db}^{w}(Q,t)$, for motile two-point dumbbells which are wiggling, calculated according to Eqs. 1 and 26 for different scattering angles. (*a*) Parameters: distance between centers $d = 1.5$ μm, mean translational speed $\langle V^2 \rangle^{1/2} = 15$ μm/s, maximum wiggle angle $A = 30°$, wiggle frequency $\nu = w_0/2\pi = 5$ s^{-1}; (*b*) same parameters as (*a*), except that $\nu = 10$ s^{-1}.

where w_0 is the wiggling frequency and A is the maximum angle. A rough characterization of observations made with a light microscope is in accord with Eq. 25; using this functional form, we will at least be able to make appropriate estimates of spectral perturbations. In all generality one needs the distribution of $\alpha(t)$ or, alternately, according to Eq. 25, one should specify the distributions of A and of w_0. However, since these are unknown, we assume in the following that A and w_0 are δ-function distributed. In Eq. 24, this corresponds to replacing the variables by their average (expected) values. In the same spirit, we set $\alpha(0) = 0$ for the sake of simplicity.
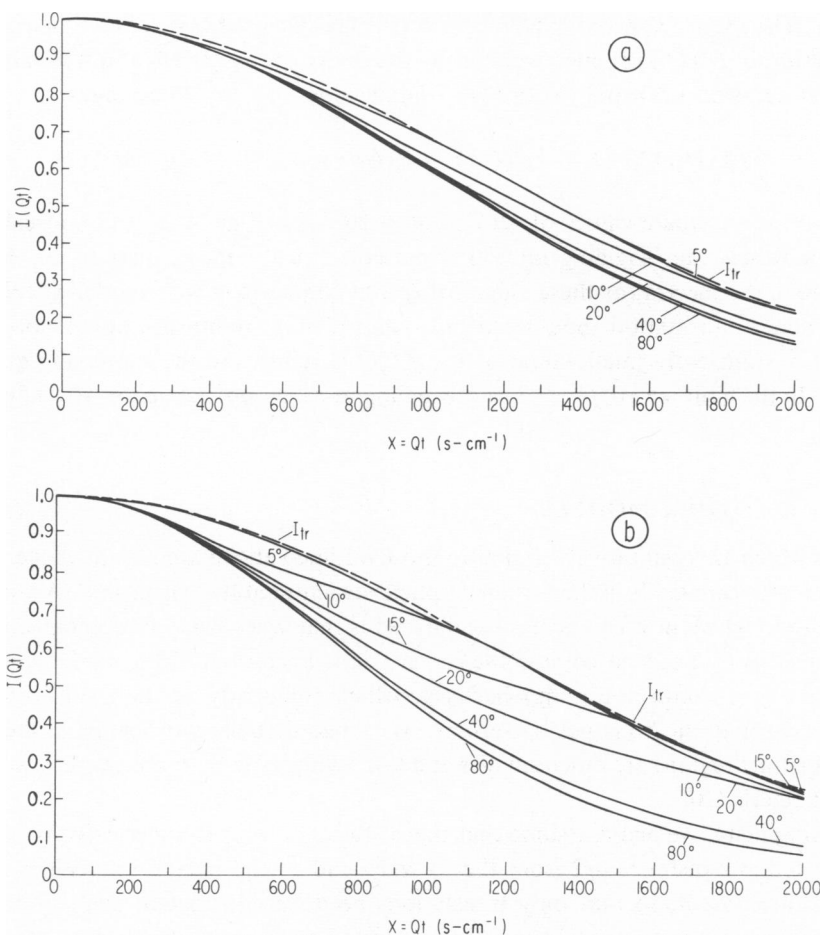
FIGURE 5 Normalized intensity correlation function $I_{\text{lin}}^{w}(Q,t)$ for a distributed line of scattering centers (see Eq. 29). Here, $b_1 = 0$, $b_2 = 1$ μm, $\langle V^2 \rangle^{1/2} = 15$ μm/s, $A = 30°$. (a) $\nu = w_0/2\pi = 5 \text{s}^{-1}$. (b) $\nu = 10 \text{s}^{-1}$. The precise values of the parameters are unimportant; for example, we could have taken $b_2 = 1.8$ μm, $A = 25°$, $\nu = 3.3$ s^{-1} and have obtained essentially the same curves as those given in Fig. 5 a. Note, also, the similarity between the expression used to compute these curves and those given in Eqs. 31 and 32.

With these approximations, Eq. 24 takes the form

$$f_{db}^{w}(Q,t) = \frac{\{1 + 2j_0(Qd) + j_0(2Qd \sin [\frac{1}{2}A \sin w_0 t])\}}{2[1 + j_0(Qd)]}. \qquad (26)$$

From this result one observes (Figs. 4, 5):

(a) When $Q \rightarrow 0$, $f^w \rightarrow 1$ so that $I(Q,t)$ probes translational motion only (see Eq. 23);

(b) For large Q, $I(Q,t)$ reflects the existence of nontranslational motion when it is

present. The spectra approximately scale as Qt. This occurs because the time scale for observation of $f^w(Q,t)$ is effectively set by the decay of $\langle j_0(QVt)\rangle$ and, for large angles, that decay occurs rapidly with t. For small values of t, Eq. 26 becomes

$$f^w_{db}(Q,t) = \{1 + 2j_0(Qd) + j_0(QdAw_0t)\}/\{2 + 2j_0(Qd)\}. \tag{27}$$

(c) For intermediate values of $Q(5° \leq \theta \leq 30°$—see Figs. 4, 5) the nonscaling of $I(Q,t)$ indicates that wiggling motion is present. Furthermore, analysis of the fine structure of the spectra for these values of Q and comparison with model calculations should reveal information about the detailed nature of the nontranslational motion.

(d) For sufficiently small values of w_0, $f^w(Q,t)$ reduces to the expression given in Eq. 27. In the limit $w \rightarrow 0, f^w \rightarrow 1$ and wiggling motions do not materially affect the spectra.

IV. OTHER MODELS

Results which are qualitatively similar to those outlined above are obtained even when major changes are made in the assumed optical structure of the bacterium. A variation of the model which now can be easily analyzed is that where only one significant scattering mass is found, located near the center of the bacterium. This model resembles vegetative (i.e. nonproliferating) bacteria, which frequently contain only one discernible chromatinic body per bacterium. We stress that the dimensions of these optically distinct regions are much smaller and less asymmetric than are those of the host E. coli bacteria (10).

For simplicity, we again assume that the scattering center is spherically symmetric, but located at a distance $b/2$ from the forward end of the bacterium. When lateral motions are absent, so that only translations need be considered, such a structure rigorously yields the correlation function given in Eq. 1, viz., $C(Qt) = \langle j_0(QVt)\rangle$ (see ref. 8). To calculate $C(Q,t)$ when wobble motions are present, we again represent the chromatinic body as a point scatterer. In this case the correlation function is calculated as in Sec. III, except that instead of Eq. 17 one has

$$B_t(Qb \mid \varphi ;\theta) = \exp[iQb \sin\{\frac{1}{2}(\alpha(t) - \alpha(0))\} \cdot \sin\theta \cdot \sin\{\varphi + \frac{1}{2}(\alpha(t) - \alpha(0))\}].$$

This term is identical to the fourth term appearing on the right hand side of Eq. 17, and, by the same arguments which lead to Eq. 24, yields $I^w_m(Q,t) = f^w_m(Q,t)$ $\langle j_0(QVt)\rangle$, where the modulation function pertaining to a medially located scattering center $f^w_m(Q,t)$ is given as

$$f^w_m(Q,t) = j_0(bQ \sin[\frac{1}{2}A \sin w_0t]). \tag{28}$$

The correlation function pertaining to a wiggling rod (i.e., a linear distribution of scattering centers which, for example, might represent a single elongated chromatinic body) also is of some interest. An *approximate* expression for this case can be obtained

from Eq. 28 if interference scattering is neglected. Let b_1 and b_2 designate the distances from the forward moving end of the bacterium to the proximal and distal scattering centers, respectively. In this case, integration of Eq. 28 yields

$$f_{\text{lin}}^{w}(Q,t) = \frac{\{\text{Si}(2b_2 Q \sin[\tfrac{1}{2}A \sin w_0 t]) - \text{Si}(2b_1 Q \sin[\tfrac{1}{2}A \sin w_0 t])\}}{2(b_2 - b_1)Q \sin[\tfrac{1}{2}A \sin w_0 t]}, \quad (29)$$

where Si($\cdots$) is the sine integral (16). Some of the approximations leading to Eq. 29 are examined in Appendix B, where optical interference between scattering centers partially is taken into account.

Despite the apparent differences in form between Eqs. 26, 28, and 29, it is interesting that, when the argument $Zb = bQ \sin[\tfrac{1}{2}A \sin(w_0 t)]$ is small, essentially equivalent expressions are obtained. We find

$$f_{db}^{w}(Q,t) \approx 1 - \frac{Q^2 d^2 \gamma_t^2}{2[1 + j_0(Qd)](3!)}; f_{m}^{w}(Q,t) \approx 1 - \frac{Q^2 b^2 \gamma_t^2}{4(3!)};$$

$$f_{\text{lin}}^{w}(Q,t) \approx 1 - \frac{Q^2 \gamma_t^2 [b_2^3 - b_1^3]}{3(3!)[b_2 - b_1]}, \quad (30)$$

where $\gamma_t \equiv 2 \sin \tfrac{1}{2} w_0 t$.

Finally, if instead of Eq. 25 one characterizes $\alpha(t)$ as $\alpha(t) = \Omega_0 t$, where Ω_0 denotes a rotational frequency, scattering functions relevant to sustained rotations can be obtained. For example, in place of Eq. 29 one finds (with $b_2 = b, b_1 = 0$))

$$f_{\text{lin}}^{\text{rot}}(Q,t) = \text{Si}\left(2bQ \sin \frac{\Omega_0 t}{2}\right) \Big/ 2bQ \sin \frac{\Omega_0 t}{2}. \quad (31)$$

Such expressions might be useful for interpreting light scattering from spinning mutants of *E. coli* or other rotating bacteria.

COMMENTS AND CONCLUSIONS

The similarity of the functions shown in Eqs. 26, 28, 29, and 31 implies the need for presupposing a particular model for nontranslational motion in order to obtain absolute measures of rotational or wiggling frequencies from inelastic light scattering data. In this regard we remark that averaging over distributions of wiggling frequencies and amplitudes also can lead to significant modification of the correlation function expressions. For example, when the modulation function for medially distributed scattering centers is averaged over a uniform distribution of frequencies ($P(w) = w_M^{-1}$ for $0 < w < w_M$; $= 0$ otherwise) we find, in place of Eq. 28,

$$f_{m}^{db}(Q,t) = \text{Si}(\tfrac{1}{2}bQAw_M t)/\tfrac{1}{2}bQAw_M t. \quad (32)$$

(For simplicity, we have presumed $w_M t$ to be small in order to derive Eq. 32, as would

be appropriate for large scattering angles [see below].) Significantly, the expression given in Eq. 32 is identical in form to that given in Eq. 31 for small $\Omega_0 t$, despite the fact that quite different assumptions have been made concerning the distribution of scattering centers and the nature of the nontranslational motion.

Nonetheless, a number of general observations can be made. First, we refer to Fig. 4, where representations of $I_{db}^w(Q,t) \equiv f_{db}^w(Q,t) \cdot I_{tr}(Q,t)$ are shown for various angles, having been computed according to Eqs. 1 and 26. The translational component $I_{tr}(Qt)$ has been computed with a Gaussian velocity distribution function having a rms speed $\langle V^2 \rangle^{1/2} = 15 \ \mu$m per s (this is approximately one-half the normal speed (7) and has been chosen to account for the reduced translational velocity resulting from the aberrant motility). In Fig. 4 a, the distance between scattering centers d was taken as 1.5 μm, the angle of maximum wiggle A was taken as 30°, and the wiggling frequency approximately 5 cps ($w_0 = 2\pi v = 30$ s^{-1}). We see that, for these parameter values, it would be difficult to discern spectral changes as the scattering angle is changed except, perhaps, at very small angles.

Although, for the latter hypothetical case, an error of approximately 30% would occur if the half maximum of $I(Q,t)$ at, e.g., $\not< 20°$, were taken as an index of translational velocity, the amplitudes and frequencies of oscillation normally observed for translating bacteria are considerably smaller than those chosen here. Thus, we can conclude that if the bacteria do not exhibit marked wobbling when viewed in the microscope, the values of swimming speed deduced from light scattering spectra are likely to be correct. In other words, for vigorous strains exhibiting strong and dominantly linear movements, wiggles and wobbles superimposed upon translational motion do not lead to significant errors when inelastic light scattering is used for measuring translational swimming speeds of bacteria (see, also, Fig. 5 a).

On the other hand, for certain aberrant cultures, spectral perturbations due to wobbling could be significant. This is illustrated in Fig. 4 b, for which parameters are identical to Fig. 4 a, except that $w_0 = 60$ s^{-1}. Variations in spectral structure, as a function of angle, are quite noticeable. Errors in determination of translational swimming speeds also would be greater.

We previously indicated that, when the bacteria are suspended in buffered media which do not support growth, they most likely would appear as uninucleate cells. In this case, correlation function expressions such as those given in Eqs. 29 or 32 would be appropriate. Consequently, we have evaluated Eq. 29 for the case $b_1 = 0$. Results, which are presented in Fig. 5, lead to qualitatively similar conclusions.

In Fig. 6 we show some normalized correlation functions which had been measured, primarily, to investigate the effect of wiggles on measurements of motility taken at intermediate scattering angles ($\sim 25°-90°$). The experimental apparatus is fully described in ref. 5, where we also discuss the relationship between "clipped" autocorrelation functions (measured by our instrument) and the functions $I(Q,t)$. The spectra pertain to a sample of $E.\ coli\ K_{12}$ bacteria which had been grown in L-broth (see ref. 5 for details) and to which glycerol had been added to a concentration of 7%. When viewed through a microscope, the sample exhibited the following features. Before
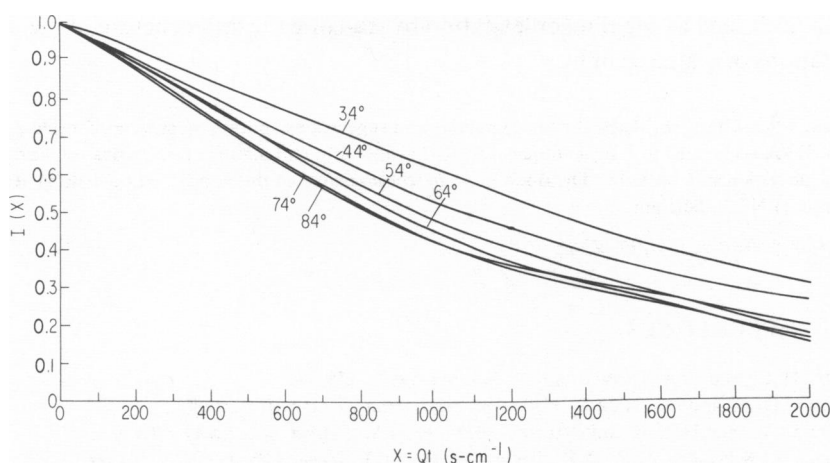
FIGURE 6   Measured intensity correlation functions for a sample of motile *E. coli* K_{12} bacteria in which wiggle motion had been effected by addition of 7% glycerol. (The channel width was 500 μs, counting rate ~500 cps, clipping level $k = 0$; see ref. 5 for further discussion.)

adding the glycerol almost all of the bacteria were moving rapidly, in apparently straight-line motion. In contrast, after the addition of glycerol almost all were wiggling markedly, and their translational motion had slowed. A broad distribution of wiggle frequencies and amplitudes were observed, the average values of which were roughly estimated to be, respectively, 2–3 s^{-1} and $A \approx 30°$. Although the scattering angle used in the present measurements does not go below 34°, some salient features are observed. In particular, we find little difference between the various spectra pertaining to larger angles, when plotted as a function of $x = Qt$ (see Fig. 6). This is in accord with the analysis shown in Figs. 4 and 5. Furthermore, the observation that the spectrum ceases to scale when the scattering angle decreases also is in agreement with theoretical predictions.[1]

We have not yet investigated how levitation occurring between linear runs contributes to the spectrum. Further investigation of this point seems desirable, in view of the possibility that such motion plays a significant role in chemotactic recognition. Although detection of nontranslational bacterial dynamics may be accomplished by stroboscopic photo-microscopy (3) or computer assisted tracking (1), quantitative measures of the details of such motion are difficult to obtain by classical light microscopy. The present work suggests the possibility of investigating components of bac-

---

[1] In a recent publication, Schaefer, Banks, and Alpert (1974. *Nature (Lond.)*. **248**:162) also present data for bacteria whose movements contain off-axial components. They study a strain of *E. coli* which, under the culture conditions used, shows considerable wobble motion when viewed through a microscope. *Qt* scaling also is a characteristic of the correlation functions which they present. Further, when they add small amounts (0.2%) of hydroxypropyl methyl cellulose to their cultures, wobble motion is suppressed. In this case the measured correlation functions decay with times which are close to those observed for wild-type strains of *E. coli* K12 grown under conditions which result in minimal nontranslation movement (7).

terial motion such as wiggling or levitation by studying the fine structure of the spectral distributions of scattered light.

REFERENCES

1. BERG, H. C., and D. A. BROWN. 1972. *Nature (Lond.).* 239:500.
2. BROWN, D. A., and H. C. BERG. 1974. *Proc. Natl. Acad. Sci. U.S.A.* 71:1388.
3. MACNAB, R., and D. E. KOSHLAND, JR. 1972. *Proc. Natl. Acad. Sci. (USA).* 64:1300.
4. TSANG, N., R. MACNAB, and D. E. KOSHLAND, JR. 1973. *Science (Wash. D.C.).* 181:60.
5. NOSSAL, R., and S-H. CHEN. 1972. *J. Phys. (Paris).* 33C1:173.
6. SCHAEFER, D. 1973. *Science (Wash. D.C.).* 180:1293.
7. NOSSAL, R., and S-H. CHEN. 1973. *Nat. New Biol.* 244:253.
8. BERNE, B. J., and R. NOSSAL. 1974. *Biophys. J.* 14:865.
9. STEMPEN, H. 1950. *J. Bacteriol.* 60:81.
10. MASON, D. J., and D. M. POWELSON. 1956. *J. Bacteriol.* 71:474.
11. WHITFIELD, J. F., and R. G. E. MURRAY. 1956. *Can. J. Microbiol.* 2:245.
12. RYTER, A. 1968. *Bacteriol. Rev.* 32:39.
13. ZUSMAN, D., A. CARBONELL, and J. HAGA. 1974. *J. Bacteriol.* 115:1167.
14. PECORA, R. 1969. *J. Chem. Phys.* 48:4126.
15. CROSS, D. A., and P. LATIMER. 1972. *Appl. Optics.* 11:1225.
16. ABRAMOWITZ, M., and I. A. STEGUN. 1964. Handbook of Mathematical Functions. National Bureau of Standards, Washington, D.C.

APPENDIX A: DERIVATION OF EQ. 19

As an example, let us consider the term (see Eqs. 15 and 16)

$$C_4 = (4\pi)^{-1} \int_0^\pi d\theta \sin\theta \int_0^{2\pi} d\varphi e^{iQVt\sin\theta\cos\varphi} e^{iE_4(\theta,\varphi)}, \tag{33}$$

where E_4 is given as

$$E_4 \equiv 2dQ \sin[\tfrac{1}{2}(\alpha(t) - \alpha(0))] \sin\theta \sin(\varphi + \tfrac{1}{2}(\alpha(t) + \alpha(0))). \tag{34}$$

The exponents in Eq. 33 may be written as

$$iQ\sin\theta[A\sin(\varphi + \epsilon) + B\cos\varphi] = iQ\sin\theta[(A\cos\epsilon)\sin\varphi + (A\sin\epsilon + B)\cos\varphi]$$
$$= iQ\sin\theta[D\cos(\varphi - \delta)], \tag{35}$$

where ϵ, A, B are defined as

$$\epsilon = \tfrac{1}{2}(\alpha(t) + \alpha(0)); \quad A = 2d\sin[\tfrac{1}{2}(\alpha(t) - \alpha(0))]; \quad B = Vt, \tag{36}$$

and δ, D are given as

$$\delta = \tan^{-1}(\cos\epsilon/(\sin\epsilon + B/A)); \quad D = [A^2 + 2AB\sin\epsilon + B^2]^{1/2}. \quad (37)$$

Thus, the fourth term on the right-hand side of Eq. 19 follows immediately from Eqs. 17 and 18 when we identify Z and φ' as $Z = QD$, $\varphi' = \pi/2 - \delta$. The other terms in Eq. 19 are derived in like fashion.

APPENDIX B: CORRELATION FUNCTIONS FOR WIGGLING RODS

We now elaborate upon the approximate expression for $f^w_{lin}(Q,t)$ given by Eq. 29. The latter was derived for a wiggling rod of scattering centers when interference scattering between centers was ignored. Its validity may be examined by employing techniques similar to those used to derive the dumbbell and point distribution correlation functions given in Eqs. 26 and 28.

Specifically, we consider the scattering mass to extend from the hinged end of the wiggling rod continuously along a line of length b (i.e., $b_1 = 0$, $b_2 = b$, see Fig. 3 and discussion preceding Eq. 29). In this case the analog of Eq. 15 is given as (cf. Eq. 2)

$$C_{lin}(Q,t) = (4\pi b^2)^{-1} \int_0^b dl \int_0^b dm \left\langle \int_0^\pi d\theta \sin\theta \int_0^{2\pi} d\varphi. \right.$$

$$\cdot \exp\{iQ\sin\theta[(-l\cos\alpha(t) + m\cos\alpha(0) - Vt)\cos\varphi$$

$$\left. + (l\sin\alpha(t) - m\sin\alpha(0))\sin\varphi]\} \right\rangle. \quad (38)$$

Thus, by arguments identical to those given in Appendix A, we have

$$C_{lin}(Q,t) = (b^{-2}) \int_0^b dl \int_0^b dm \langle j_0(Q\tilde{D}(m,l)) \rangle \quad (39)$$

where $\tilde{D}(m,l)$ is defined as

$$D = \{l^2 + m^2 - 2lm\cos(\alpha(t) - \alpha(0))$$

$$+ 2Vt[l\cos\alpha(t) - m\cos\alpha(0)] + (Vt)^2\}^{1/2}. \quad (40)$$

Using the addition theorem given in Eq. 21 we find

$$C_{lin}(Q,t) \simeq I_{lin}(Q,t) \langle j_0(QVt) \rangle,$$

where $I_{lin}(Q,t)$ is given as

$$I_{lin}(Q,t) = (b^{-2}) \int_0^b \int_0^b \langle j_0(Q[l^2 + m^2 - 2lm\cos(\alpha(t) - \alpha(0))]^{1/2}) \rangle \, dl\, dm \quad (41)$$

$$= (2b^{-2}) \int_0^b dl \int_0^l dm \langle j_0(Q[(\beta_t l)^2 + m^2 - m(l\beta_t)\beta_t]^{1/2}) \rangle, \quad (42)$$

with β_t defined as in Eq. 20. (Eq. 42 follows from Eq. 41 by a change of variables, taking account of the fact that the integrand in Eq. 41 is symmetric in l, m.)

Further analytical reduction of Eq. 42 is in general difficult to achieve. However, if β_t is small we can write

$$j_0(Q[(\beta_t l)^2 + m^2 - m(l\beta_t)\beta_t]^{1/2}) \simeq j_0(Q\beta_t l)j_0(Qm),$$

so that Eq. 42 becomes

$$I_{\text{lin}}(Q,t) \simeq 2(bQ)^{-2} \left\langle \int_0^{bQ} dz\, j_0(\beta_t z) \int_0^z dy\, j_0(y) \right\rangle \qquad (43)$$

$$= 2(bQ)^{-2} \left\langle \sum_{k=0}^{\infty} C_k \beta_t^{2k} f_k(bQ) \right\rangle, \qquad (44)$$

with the $\{C_k\}$ and $\{f_k(bQ)\}$ given as

$$C_k = (-1)^k/(2k + 1)(2k + 1)! \qquad (45)$$

and

$$f_k(bQ) = (bQ)^{2k+1}\,\text{Si}(bQ) - \int_0^{bQ} z^{2k} \sin z\, dz. \qquad (46)$$

For large bQ, one has $(bQ)^{2k+1}\,\text{Si}(bQ) \approx (\pi/2)(bQ)^{2k+1}$ and $\int_0^{bQ} z^{2k} \sin z\, dz = \mathcal{O}(bQ)^{2k}$. Thus, a good approximation is obtained by neglecting the integral terms in Eq. 46, in which case one has

$$I_{\text{lin}}(Q,t) \simeq 2\,\frac{\text{Si}(bQ)}{bQ} \left\langle \sum_{k=0}^{\infty} \frac{(-1)^k(\beta_t bQ)^{2k}}{(2k + 1)(2k + 1)!} \right\rangle \qquad (47)$$

$$\equiv 2\,\frac{\text{Si}(bQ)}{bQ} \cdot f_{\text{lin}}^w(Q,t), \qquad (48)$$

where $f_{\text{lin}}^w(Q,t)$ is the (normalized) spectral modulation due to wiggling. After averaging according to Eq. 25, the series may be summed to give

$$f_{\text{lin}}^w(Q,t) = \frac{\text{Si}(2bQ \sin[(A/2)\sin w_0 t])}{2bQ \sin[(A/2)\sin w_0 t]}. \qquad (49)$$

This expression reduces to that given in Eq. 29 with $b_1 = 0$, $b_2 = b$.